Eur. J. Mineral.
2009, **21**, 571–580
Published online April 2009

Compression behaviour and flexibility window of the analcime-like feldspathoids: experimental and theoretical findings

G. DIEGO GATTA[1,2,*], ASEL SARTBAEVA[3] and STEPHEN A. WELLS[4]

[1] Dipartimento di Scienze della Terra, Universita' degli Studi di Milano, Via Botticelli 23, I-20133 Milano, Italy
*Corresponding author, e-mail: diego.gatta@unimi.it
[2] CNR-Istituto per la Dinamica dei Processi Ambientali, Milano, Italy
[3] Department of Chemistry, Inorganic Chemistry Laboratory, University of Oxford, South Parks Road, Oxford OX1 3QR, UK
[4] Department of Physics and Centre for Scientific Computing, University of Warwick, Gibbet Hill Road, Coventry CV4 7AL, UK

Abstract: The analcime-like feldspathoids are a group of microporous minerals with the ANA framework topology. Analcime proper has predominantly Na as its channel cation content, while leucite contains predominantly K and wairakite contains Ca. Under compression, all three minerals display structural phase transitions to lower-symmetry forms. In cubic analcime the phase transition occurs at a relatively low pressure (~1 GPa). Our recent theoretical study using geometric simulation indicates that this phase transition is controlled by the flexibility window of the ANA framework. The flexibility window is defined as the range of ''framework densities'' over which the tetrahedral units of the framework can in principle be made geometrically ideal. In leucite and wairakite the ambient-pressure structure is more distorted than in analcime, due to the different cation content, and their subsequent phase transitions occur at higher pressures (~2–3 GPa). We discuss the experimental data for these minerals and its relationship to the theoretical flexibility of the ANA framework and to the influence of cation content.

Key-words: analcime, leucite, wairakite, feldspathoids, high-pressure, compressibility, flexibility window, phase transition, geometric simulation.

1. Introduction

Analcime (or analcite, ideal chemical formula: $Na_{16}Al_{16}Si_{32}O_{96}\cdot 16H_2O$), leucite ($K_{16}Al_{16}Si_{32}O_{96}$) and wairakite ($Ca_8Al_{16}Si_{32}O_{96}\cdot 16H_2O$) are commonly defined as feldspathoids, although the Commission of the International Mineralogical Association included those into the zeolites group (Coombs *et al.,* 1997). In nature, analcime occurs in a wide variety of geological environments, as a primary and secondary mineral (Roux & Hamilton, 1976; Woolley & Symes, 1976; Wilkinson, 1977; Luhr & Kyser, 1989; Gianpaolo *et al*., 1997; Redkin & Hemley, 2000; Prelević *et al*., 2004). Primary analcime has rarely been found (in rocks like blairmorites or minettes, Wolley & Symes, 1976; Wilkinson, 1977; Luhr & Kyser, 1989), in contrast a wide number of secondary analcimes has been found as product of alteration of primary magmatic minerals (*e.g.*, nepheline and leucite, Gianpaolo *et al*., 1997; Redkin & Hemley, 2000; Prelević *et al*., 2004 and references therein). Leucites occur as primary minerals in volcanic rocks, in particular potassium-rich mafic and ultramafic rocks (*e.g.*, leucite-basanites, leucite-tephrites, leucite-phonolites, leucite-melilite basalts, ugandites and katungites, Peccerillo, 1998, 2003, 2005; Deer *et al*., 2004). Wairakite is a rare mineral, and occurs in low-grade metamorphic environments or in areas with hydrothermal activities (Gottardi & Galli, 1985; Tschernich, 1992; Armbruster & Gunter, 2001; Passaglia & Sheppard, 2001).

Analcime, leucite and wairakite are isotypic (or homeotypic) minerals and with pollucite ($Cs_{12}Na_4Al_{16}Si_{32}O_{96}\cdot 12H_2O$) and hsianghualite ($Li_{16}Ca_{24}Be_{24}Si_{24}O_{96}F_{16}$) belong to the so called ''analcime group'' (Gottardi & Galli, 1985; Armbruster & Gunter, 2001; Baerlocher *et al*., 2001). The crystal structure of this group of isotypic open-framework silicates results from the combination of two ''secondary building units'' (SBU), constituted by 4 and 6-membered rings of tetrahedra (Baerlocher *et al*., 2001) (Fig. 1). The framework topology (*i.e.*, ANA topology, Baerlocher *et al.*, 2001) shows the maximum symmetry ($Ia\bar{3}d$). Two different systems of channel can be observed in such a framework type: irregular channels formed by highly distorted 8-membered rings (8 mR) and regular channels formed by 6-membered rings (6 mR) along the [111] direction of the cubic lattice. The general

DOI: 10.1127/0935-1221/2009/0021-1923
0935-1221/09/0021-1923 $ 4.50

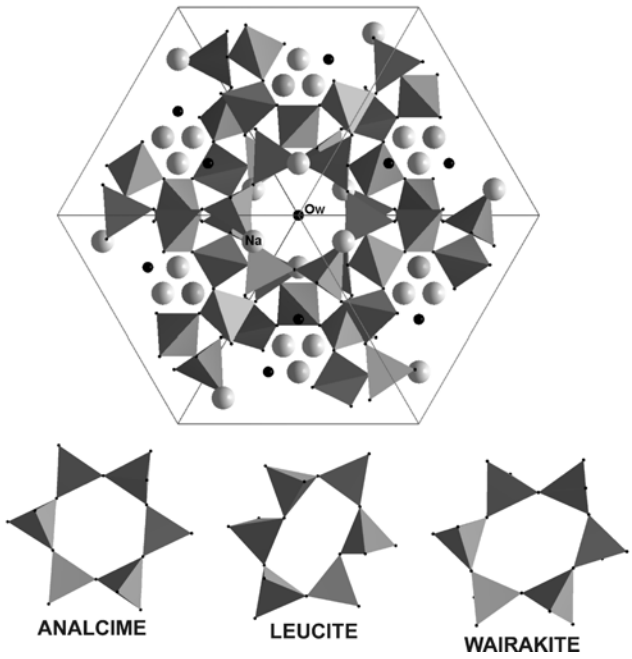

Fig. 1. (*Above*) Crystal structure of cubic analcime viewed down [111] and (*below*) configuration of the 6-membered rings in analcime, leucite and wairakite at room conditions.

symmetry of the minerals belonging to the analcime-group is usually lower than the framework symmetry, due to the Si/Al-ordering of the tetrahedral framework and to the extra-framework content. In analcime, the extra-framework population is represented by Na^+ and H_2O molecules. In cubic analcime (space group: $Ia\bar{3}d$), there is a statistical Si/Al-distribution in the tetrahedral framework and the Na sites are statistically 2/3 occupied (for charge balance). The Na sites are 6-coordinated (with four oxygens belonging to the tetrahedral framework and two to the water molecules) and lie in the framework voids (Ferraris *et al*., 1972; Gatta *et al*., 2006). Evidence of non-cubic analcime was reported in the literature (Gatta *et al*., 2006 and references therein). The reason for the different symmetries is still unclear; however, different degrees of ordering in the Si/Al distribution might be one of the explanations. (Mazzi & Galli, 1978; Hazen & Finger, 1979; Gatta *et al*., 2006). In leucite, a disordered Si/Al-distribution at room condition is observed (Mazzi *et al*., 1976; Gatta *et al*., 2008 and references therein). The extra-framework content is represented only by K, which is located at the same site occupied by H_2O in the analcime structure, forming a distorted polyhedron with six K—O bond-distances between 2.96 and 3.14 Å and six distances between 3.50 and 3.76 Å (Mazzi *et al*., 1976; Gatta *et al*., 2007, 2008). The general symmetry of leucite is tetragonal (space group: $I4_1/a$). In wairakite, there is an almost ordered Si/Al-distribution in the tetrahedral sites and at least six extra-framework sites occur: two are fully occupied by water molecules and four by cations (Ca + Na) (Takeuchi *et al*., 1979; Ori *et al*., 2008). Wairakite and analcime are two hydrous members of the analcime-group and show a similar arrangement of the extra-framework population, with regular (Ca, Na)-octahedra formed by two water molecules at the apices and four framework oxygens. The general symmetry of wairakite is monoclinic (space group: $I\,2/a$).

Several studied have been devoted to the behaviour of analcime, leucite and wairakite under non-ambient conditions, reported in Gatta *et al.* (2006), Gatta *et al.* (2008) and Ori *et al.* (2008), respectively. In particular, the high-pressure (H*P*) behaviour of analcime and leucite has been recently investigated by *in situ* X-ray single-crystal diffraction with a diamond anvil cell (DAC) up to ~7 GPa (Gatta *et al*., 2006, 2008) and that of wairakite by *in situ* synchrotron powder diffraction up to ~7.8 GPa with a DAC (Ori *et al.*, 2008) under hydrostatic regime. All the three minerals experienced a phase-transition from high-symmetry to low-symmetry polymorph at high-pressure: 1) analcime, between 0.91(5)–1.08(5) GPa from $Ia\bar{3}d$ to $P\bar{1}$ symmetry; 2) leucite, between 2.19(4)–2.77(1) GPa from $I4_1/a$ to $P\bar{1}$ symmetry; 3) wairakite, between 2.5(1)–3.2(1) GPa from $I2/a$ to $P\bar{1}$ symmetry. For analcime and leucite, the *P*-induced phase-transition is unambiguously a first-order transition; in contrast, for wairakite the order of the transition cannot be unambiguously defined, mainly because of the quality of the powder data. Gatta *et al.* (2006) provided the structure refinement of the low-*P* and high-*P* polymorphs of analcime, showing the *P*-induced phase-transition at ~1 GPa is displacive in character. For leucite and wairakite, the *P*-induced structural evolution of the low-*P* polymorphs was described (Gatta *et al*., 2008; Ori *et al*., 2008), whereas the crystal-structure and the structure-evolution of the high-*P* polymorphs are still unknown.

The aim of this study is to compare the elastic behaviour and the *P*-induced structural evolution of the aforementioned isotypic minerals on the basis of the previous experimental data and geometric simulation, in order to define the role played by the framework (*i.e.*, Si/Al-ordering, distortion of the 6 mR at ambient conditions) and extra-framework content (nature of the cations and ionic valence, ionic radii, coordination number, presence of water molecules). A recent theoretical study using geometric simulation indicates that *P*-induced phase transition is controlled by the ''flexibility window'' (described later in the paper) of the cubic ANA structure (Sartbaeva *et al*., 2008). We discuss the experimental data for these minerals and its relationship to the theoretical flexibility of the ANA framework and to the influence of cation content.

2. Experimental: comparative compressibility

In order to compare the elastic parameters of analcime, leucite and wairakite, axial (''linear'') and volume compressibility (as ''linearised'' and volume bulk moduli) have been calculated using a Birch-Murnaghan Equation-of-State (BM-EoS) (Birch, 1947; Angel, 2000). The BM-EoS is based upon the assumption that the *P*-induced

strain energy of a solid can be expressed as a Taylor series in the Eulerian strain,

$$f_e = [(V_0/V)^{2/3} - 1]/2$$

(V_0 and V represent the cell volume, or molar volume, under room and H*P* conditions respectively). Expansion in the Eulerian strain polynomial has the following form:

$$P = 3K_0 f_e(1 + 2f_e)^{5/2}\{1 + 1.5(K' - 4)f_e + 1.5 \times [K_0K'' + (K' - 4)(K' - 3) + 35/9]f_e\} + \ldots,$$

where K_0 represent the bulk modulus ($K_0 = -V_0(\partial P/\partial V)_{P0} = 1/\beta$; β is the volume compressibility coefficient, $K' = (\partial K_0/\partial P)$ and $K'' = (\partial^2 K_0/\partial P^2)$. The same EoS, as that used to fit the *P*-*V* data, can be used to describe the axial compressibilities by substituting the cube of lattice parameter for the volume (''linearised EoS'', Angel, 2000). The ''linear-K_0'' obtained in this way is related to the axial compressibility (β_j) by:

$$\beta_j = -1/(3K_{0j}) = 1/l_{0j}(\partial l_j/\partial P),$$

where l_{0j} ($j = a, b, c$) is the length of the unit-cell axis under room conditions.

Volume and axial compressibility of analcime, leucite and wairakite were calculated with the EOS-FIT5.2 computer program (Angel, 2001), with data weighted by the uncertainties in P (± 0.05 GPa for single-crystal and ± 0.10 GPa for powder experiments) and V (or a, b, c). The unit-cell parameters of the three feldspathoids at different pressures are reported in Gatta *et al.* (2006, 2008) and Ori *et al.* (2008). For the low-*P* polymorphs, the best EoS-fit was achieved adopting a truncated second-order BM-EoS (*i.e.*, with K' fixed to four). For the high-*P* polymorphs, a second-order BM-EoS was used to describe the compressional behaviour of leucite and wairakite, whereas a third-order BM-EoS was adopted for analcime (*i.e.*, with $K' \neq 4$). The refined elastic parameters by EoS-fit are reported in Table 1. The volume BM-EoS fit are shown in Fig. 2. The elastic anisotropy is reported as a ratio between the axial bulk moduli (Table 1).

Eulerian strain *vs.* ''normalised pressures'' plots (*fe-Fe* plot, Angel, 2000) for analcime, leucite and wairakite are reported in Fig. 3 and the weighted linear regressions through the data-points, for the low-*P* and high-*P* polymorphs, are shown. The almost horizontal weighted linear regression support the second-order BM-EoS used for low-*P* and high-*P* polymorphs of leucite and wairakite (Angel, 2000). The calculated *Fe*(0) values agree with the K_0 values obtained by the EoS-fit (Table 1).

3. Experimental: *P*-induced structural evolution

The H*P*-crystal structure evolution of analcime, leucite and wairakite was studied on the basis of several structural refinements at different pressures. For analcime, Gatta *et al.* (2006) were able to solve the crystal structure of the high-*P* polymorph and to describe the structural evolution of the triclinic polymorph, whereas for leucite and wairakite only the *P*-induced structure evolution of the low-*P* polymorphs (*i.e.*, tetragonal and monoclinic, respectively) were described.

The main deformation mechanisms with *P* observed for the low-*P* polymorphs of the three isotypic feldspathoids consist of polyhedral tilting. The tetrahedra behaved as rigid building block units, as shown by the evolution of the bond-distances and angles (Gatta *et al.*, 2006, 2008; Ori

Table 1. Elastic parameters based on the axial and volume BM-EoS fit for the low- and high-*P* polymorphs of analcime, leucite and wairakite.

	Analcime (low-*P*)	Analcime (high-*P*)	Leucite (low-*P*)	Leucite (high-*P*)	Wairakite (low-*P*)	Wairakite (high-*P*)
Space group	$Ia\bar{3}d$	$P\bar{1}$	$I4_1/a$	$P\bar{1}$	$I2/a$	$P\bar{1}$
K_a (GPa)		29(2)	34.5(5)	35.9(5)	36(1)	50(6)–76(7)[a]
K_a'		4.9(6)	4	4	4	4
β_a (GPa^{-1})	0.0059(3)	0.0115(8)	0.0097(2)	0.0093(2)	0.0093(3)	0.0067(8)–0.0044(4)[a]
K_b (GPa)		20(1)	–	34.9(7)	70(5)	112(19)–159(20)[a]
K_b'		5.2(5)	–	4	4	4
β_b (GPa^{-1})		0.0167(8)	–	0.0096(3)	0.0048(5)	0.0030(5)–0.0021(3)[a]
K_c (GPa)		11(1)	78(1)	35.5(7)	26(1)	7(1)–26(1)[a]
K_c'		12.6(6)	4	4	4	4
β_c (GPa^{-1})		0.030(3)	0.0043(1)	0.0094(2)	0.0128(5)	0.048(6)–0.0129(3)[a]
K_a:K_b:K_c		2.64:1.82:1	1:1:2.26	1.03:1:1.02	1.38:2.69:1	2.92:6.11:1[a]
V_0 (Å^3)	2571.2(4)	2607(9)	2351.1(1)	2317(3)	2536(4)	2632(38)
K_0 (GPa)	56(3)	19(2)	41.9(6)	33.2(5)	39(3)	24(3)
K'	4	6.8(7)	4	4	4	4
β_V (GPa^{-1})	0.018(1)	0.053(6)	0.0239(4)	0.0301(5)	0.026(2)	0.042(5)
Fe(0) (GPa)	–	19.2(2)	42(1)	33.2(4)	33(7)	23(1)

[a]Elastic parameters calculated adopting a weighted linear regression through the data points. For triclinic wairakite, the axial EoS-fits are significantly poor.

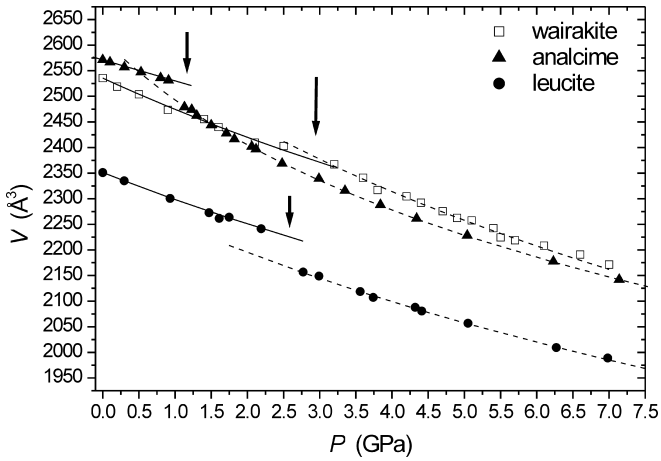

Fig. 2. Variation as a function of P of the unit-cell volume of analcime, leucite and wairakite, and EoS-fits for low-P (solid lines) and high-P polymorphs (dotted lines). The *e.s.ds* values are slightly smaller than the size of the symbols. The arrows indicate the transition pressure from the high-to-low symmetry form of the three feldspathoids.

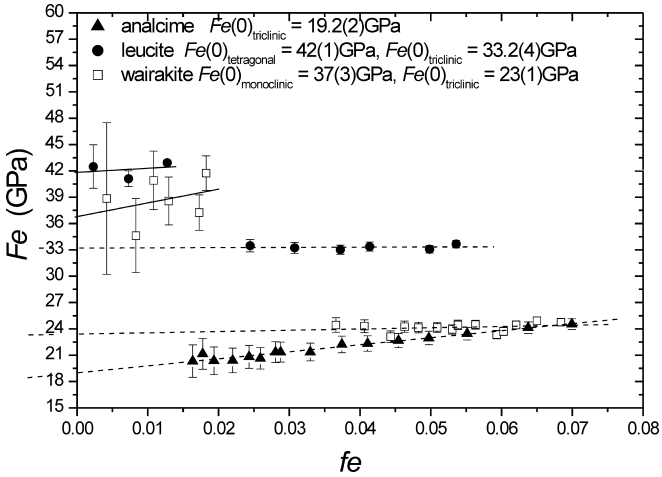

Fig. 3. Plot of the Eulerian finite strain ($f_e = [(V_0/V)^{2/3} - 1]/2$) *vs.* the normalised stress ($F_e = P/[3f(1 + 2f)^{5/2}]$) for the high-$P$ polymorphs of analcime and low- and high-P polymorphs of leucite and wairakite. For the HP-polymorphs, the strain values were calculated using the V_0 value obtained from the BM-EoS fit. The *e.s.ds* were calculated according to Heinz & Jeanloz (1984). The weighted linear regressions through the data points are shown (solid lines for the low-P polymorphs, dotted lines for the high-P polymorphs).

et al., 2008). The 6 mR of tetrahedra (along the [111] of the idealised cubic framework) cannot be deformed in cubic analcime, because of the symmetry, but show significant changes in leucite and wairakite. Upon increasing pressure, the independent 6 mRs in leucite grow more elliptic, as shown by the significant decrease of the ''ellipticity ratio'' (*i.e.*, shortest/longest diameters of the ring; the higher the ellipticity ratio, the lower the ellipticity; for an ideal and undistorted 6 mR, the ellipticity ratio is one) (Gatta *et al*., 2006, 2008). As reported by Gatta *et al.* (2008), the compression of the 6 mR seems to govern the drastic elastic anisotropy of the tetragonal leucite structure, as shown by the different values of the axial bulk moduli ($K_c = 78(1)$ and $K_a = 34.5(5)$ GPa, Table 1). In monoclinic wairakite, the two independent and deformable 6 mRs show a conflicting behaviour with P, as one shows a monotonic decrease of the ellipticity ratio whereas the other shows an increase (Ori *et al*., 2008). The 4 mR of tetrahedra, a further secondary building unit of the ANA-type framework (Baerlocher *et al*., 2001), behaves as a rigid unit in cubic analcime, because of the symmetry. In tetragonal leucite, there are three independent 4 mRs. Two of them behave as rigid units at high-P because of the symmetry, they cannot deform and their ellipticity ratio is one at any given P. The third one, in contrast, is a deformable unit and its ellipticity ratio decreases monotonically with P (Gatta *et al*., 2008). In monoclinic wairakite, four independent 4 mRs behave as deformable units: two of them show a monotonic increase of the ellipticity ratio and the other two a non-monotonic trend with P (Ori *et al*., 2008). The extra-framework content does not show any relevant change within the stability field of the low-P polymorphs, as shown by the atomic-position and bond-distances (*i.e.*, Na—O, Na—H_2O, K—O, Ca—O, Ca—H_2O, Gatta *et al*., 2006, 2008; Ori *et al*., 2008). A homogeneous compression without any relevant distortion of the extra-framework polyhedra was observed for all the low-P polymorphs.

We would emphasise that the symmetry restrictions on the 6 mR and 4 mR units of analcime and leucite are restrictions on the *average* atomic positions in the crystal. It is typical of flexible framework structures for there to be differences between the average high-symmetry structure and the instantaneous local structure, a point which we examine in more detail in the theoretical section.

The structure refinements at different pressure of the high-pressure triclinic polymorph of analcime show that: 1) a Si/Al-statistical distribution is maintained (as in cubic analcime) up to the maximum pressure achieved, based on the tetrahedral bond distances and angles, 2) the atomic relaxation mainly occurs through a tetrahedral tilting and 3) a strong deformation mechanism of the Na-polyhedra in response to the applied pressure occurs. The first-order cubic-to-triclinic phase-transition in analcime is displacive in character, and completely reversible. The HP-polymorph of analcime is crystalline at least up to 7 GPa. The P-induced phase-transition leads to a significant distortion of the tetrahedral framework. In cubic analcime, the 6 mR along [111] is an ideal hexagonal ring with inter-tetrahedral T—O—T angle of about 143.4°. At $P \sim 1.2$ GPa, the triclinic structure shows strongly deformed 6 mRs, with some T—O—T angle of about 128° (Gatta *et al.,* 2006). The ellipticity ratio of the 6 mRs tends to decrease monotonically with P. At pressures above the cubic-to-triclinic phase-transition, the configuration of the extra-framework content changes. In cubic analcime, the coordination number (CN) of the Na site is six (four oxygens belonging to the tetrahedral framework and $2H_2O$). At $P \sim 1.2$ GPa, the structure refinement shows that eight Na sites have a CN = 6 and four Na sites have a CN = 7; at $P \sim 5$ GPa, four Na sites show

CN = 6, seven Na sites CN = 7 and one Na site CN = 8 (Gatta *et al*., 2006). In other words, the compression of the voids leads to an increase of the coordination number of the Na sites.

4. Theoretical: geometric simulation of frameworks

Geometric simulation is a simplified method for modelling the behaviour of flexible framework structures such as silicates and aluminosilicate zeolites. Most conventional simulation methods represent atomic interactions using two- and three-body interaction energy terms. In geometric simulation the bonding constraints in a group of atoms (in this case a tetrahedron) are represented using a template or ''ghost'', which has the ideal geometric shape of the group (T—O bond and O—T—O bond angles). During the simulation the ghost moves and rotates to match the overall position and orientation of the group, while each atom is joined by a constraint to a single vertex of the ghost. Over multiple iterations the positions of the ghost and of the atoms change so as to match each other as close as possible. This form of multi-body collective interaction is particularly suitable for framework materials, where an important contribution to the dynamics comes from collective quasi-rigid motion of the tetrahedral units. Details of the method and its applications to mineral and biological structures have been given previously (Wells *et al.,* 2002, 2004, 2005; Sartbaeva *et al*., 2004, 2005, 2006). This simplified modelling technique, which takes account of only short-range bonding and contact forces is complementary to more detailed simulation methods using interatomic potentials or *ab initio* techniques.

We have previously applied geometric simulation to investigate the compression mechanisms of the zeolites edingtonite and levyne (Gatta & Wells, 2004, 2006). The method in these studies was to begin from the experimentally determined structure at ambient conditions and simulate compression by altering the unit-cell parameters and using geometric simulation to update atomic positions. By simulating different hypothetical modes of compression for the structure, we were able to account for the observed high-pressure behaviour. These two zeolites have highly anisotropic structures with well-defined secondary building units and relatively low ''framework densities'' [*i.e.*, the number of tetrahedrally coordinated atoms (T-atoms) per 1000 $Å^3$, Baerlocher *et al*., 2001] of the order of 15–16 T/1000 $Å^3$. The geometric simulation easily identified the principal compression modes in terms of tetrahedral tilting (Gatta & Wells, 2004, 2006).

We have also applied geometric simulation to define the ''flexibility window'' (Sartbaeva *et al*., 2006) as a property of zeolite frameworks. The flexibility window is a range of densities over which the corner-sharing TO_4 units making up the zeolite framework can in principle be made perfectly tetrahedral. This window is limited at high density by contacts between oxygen atoms on neighbouring tetrahedral units, and at low density by extension of the T—O bonds (though not, in general, by linear T—O—T angles). High-silica zeolites are found experimentally to exist at the low-density end of the window, indicating that zeolites are maximally extended structures. In a recent study we demonstrated that the flexibility window of the cubic ANA framework controls the pressure induced phase transition in analcime (Sartbaeva *et al*., 2008).

We have now performed an extensive geometric modelling study of analcime, leucite and wairakite. We discuss these results in terms of both the flexibility windows of cubic and non-cubic ANA framework, and also the tetrahedral tilting compression mechanisms.

5. Theoretical: flexibility windows in the ANA framework

In a previous study we performed geometric simulations on a series of zeolite frameworks using tetrahedral templates appropriate to pure silica (Si—O bond length of 1.61 Å) (Sartbaeva *et al*., 2006). We simulated a range of densities by controlling the unit-cell parameters in the simulations, and used geometric relaxation to determine whether the SiO_4 tetrahedra could be made geometrically perfect, or whether distortions were intrinsic to the structure. From theory it was unclear whether we should expect the polyhedra to be perfectible at any density. Indeed, we found that several proposed hypothetical tetrahedral framework structures were intrinsically strained and the tetrahedra could not be made ideal at any density. Strikingly, however, all of the zeolite frameworks which we examined (naturally occurring or synthetic) were perfectible, not only at a single point but over a range of densities. Furthermore, we were able to compare our simulations to experimental data for zeolites which exist in high-silica forms, finding that these structures are found experimentally to lie at the low-density edge of the perfectible range. This result led us to define the term ''flexibility window'' to describe the range of densities over which a framework is perfectible, and to suggest that the possession of a flexibility window is a defining characteristic of a zeolite framework.

During this study we simulated a cubic ANA framework as pure silica. Curiously, cubic ANA had both the highest framework density of the zeolites that we examined, and also displayed the narrowest flexibility window; the framework could be compressed by only 3 % in volume before oxygen atoms came into contact. This led us to examine a possible connection to the unusual high-pressure behaviour of cubic analcime.

We therefore performed further simulations as described in Sartbaeva *et al.* (2006) using a tetrahedral geometry appropriate to the Si:Al ratio of natural cubic analcime – 2.3:1 in this case. This corresponds to a T—O bond length of 1.65 Å. We used this average bond length as there is no evidence of Si/Al ordering in this structure. These simulations produced data that we could compare directly to the observed cell volumes during the compression of cubic analcime.

We initially performed simulations of the framework with the cubic unit-cell parameters observed during the experiment and found that the structures are perfectible over the whole observed range of cubic analcime, from ambient conditions up to around 1 GPa. Interestingly, the much lower-symmetry triclinic structure observed after the phase transition is also perfectible; on further compression, however, the structure passes out of the window and distortions of the framework are inevitable.

We obtained the theoretical limits of the flexibility window in cubic analcime by simulations setting the cubic cell parameter outside the range observed in the experiment. As expected, we found that the low-density edge of the window lies near the density observed for the structure at ambient conditions, confirming that the ambient structure is close to maximal extension.

Interestingly, we found that the high-density edge of the window on compression lies near the last observed cubic structure before the transition. Simulation of tetragonal and orthorhombic distortions of the cubic cell near the high-density edge of the window indicated that only very small variations in density could be achieved before distortions of the polyhedra became inevitable. The sudden transition from the highly symmetric cubic form to the low-symmetry triclinic form may thus be explained; the structure reduces its volume while remaining perfectible, which cannot be achieved by transition to intermediate-symmetry forms. These results for analcime are summarised in Fig. 4.

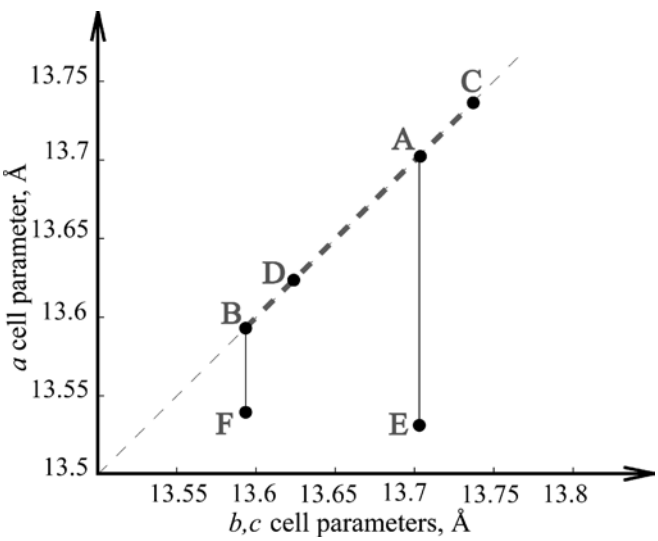

Fig. 4. Flexibility window for cubic/tetragonal analcime framework depending on cell parameters. Metrically cubic structures lie along the diagonal (thin dashed) line. Point ''A'' shows the structure at ambient conditions; ''B'' and ''C'' – high and low density edges of the flexibility window for the cubic cell; ''D'' – last experimental point on compression of the cubic analcime. The thick dashed line from B to C is the flexibility window of cubic analcime. ''E'' and ''F'' points indicate high density edges of the flexibility window for tetragonal distortions of analcime, where the *a* parameter only is compressed, starting from the ambient and most-compressed cubic points respectively.

If we are correct about the significance of the flexibility window for zeolite frameworks, we should expect that the ANA framework will also be perfectible with the parameters of leucite and wairakite in their low-pressure forms. We would also expect that the framework will cease to be perfectible near the transition to the high-pressure forms. We can test this prediction by geometric simulations using the experimental data from Gatta *et al.* (2008) for leucite and Ori *et al.* (2008) for wairakite. Both of these structures displayed an Si:Al ratio close to 2:1 and we therefore performed our geometric simulation with the same 1.65 Å T–O bond length as for analcime.

The leucite framework was observed experimentally to be tetragonal ($I4_1/a$) from ambient pressure up to 2.4 GPa, where a first-order displacive phase transition occurred to a low-symmetry triclinic ($P\bar{1}$) form. This behaviour is very similar to that observed for the cubic analcime. Our geometric simulations found that the tetragonal framework was perfectible at all of the cell volumes observed in the low-pressure form; it is thus clear that all these points lie within a flexibility window for the tetragonal ANA framework. The framework is not perfectible in the high-pressure form, although the intrinsic distortion at the first high-pressure data point is very small. It thus appears that the phase transition in leucite has the same character as that in analcime, with the structure remaining in the tetragonal form until it is no longer perfectible and then making the transition to a low-symmetry form.

Wairakite was observed to transform from a monoclinic (*I2/a*) to a lower-symmetry form ($P\bar{1}$) between 2.5 and 3.2 GPa (Ori *et al.,* 2008). This study was performed using powder X-ray diffraction rather than single-crystal as for the leucite and analcime data, and the order of the transition is not clear. We again performed geometric simulations using the cell parameters for each data point, finding that the monoclinic framework is perfectible up to 0.9 GPa, after which distortions become inevitable. We note that, unlike leucite and analcime, wairakite displays a degree of Si/Al ordering in the framework, which may account for the discrepancy between the onset of distortion in our simulations and the position of the observed transition. We are currently pursuing a more detailed simulation study of ordered wairakite.

Our findings for the perfectibility of the ANA framework in each of these different crystal structures are summarised in Fig. 5. This figure shows the same *P-V* data as in Fig. 2, with the data points labelled according to whether the structure is perfectible or not.

The pattern for analcime and leucite is clear; for the low-pressure structures the framework is perfectible, and the transition to the high-pressure, low-symmetry form is associated with the onset of inevitable distortions in the framework. In wairakite the association with the phase transition is less clear, but we still find that the framework at ambient conditions is perfectible.

We emphasise that when we describe the structure as ''perfectible'' we are describing a *geometric* property, *i.e.* that the framework atoms can in principle be arranged into a network of exactly corner-sharing regular tetrahedra

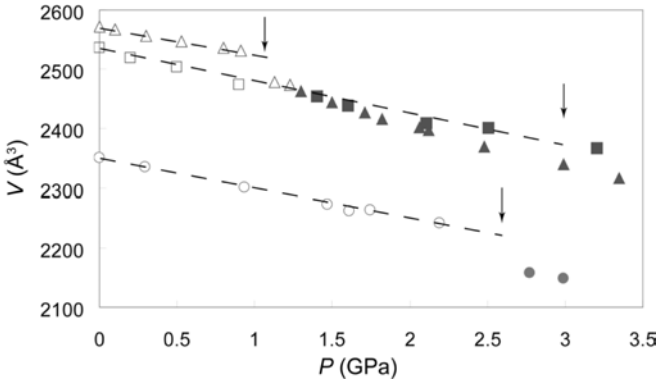

Fig. 5. *P*-*V* data for analcime (triangles), wairakite (squares) and leucite (circles), as for Fig. 2. Symbols are open where the framework is perfectible and closed where the framework is intrinsically distorted. For analcime the cubic form is perfectible as are the first two points for the triclinic structure. Leucite is perfectible in the tetragonal form and not in the triclinic form. Wairakite is perfectible at low pressures and then becomes intrinsically distorted at very similar *P* and *V* values to cubic analcime.

with the given T–O bond length. This is not a claim that the actual atomic positions display this perfect geometry, either instantaneously or on average. What, then, is the physical significance of this property? Consider a division of the atomic interactions in the zeolite into most-local (bonding and steric contact) terms U_b, which favour ideal tetrahedral geometry for TO_4 units, and longer-range terms (for example dispersion and electrostatic interactions) U_l. Distortions of the TO_4 units arise from a trade-off between U_b and U_l terms. Geometric simulation is equivalent to the introduction of only the U_b terms. If the structure lies within the flexibility window, it can reach the global minimum for the energy of the U_b terms. The energy cost for small distortions of the TO_4 units, when we introduce the U_l terms, is then minimal and second-order. If, on the other hand, the structure is outside the flexibility window, it cannot reach the global minimum for the U_b terms, as the TO_4 units are intrinsically strained. Therefore, the energy cost for further distortions of the TO_4 units, when we introduce the U_l terms, is obviously higher and first-order.

The channel contents of zeolites are of unquestioned importance in determining the minerals' physico-chemical properties. However, it should now be clear that the nature of the interactions between the framework and the channel contents depends on whether the structure lies within its flexibility window or not. The examination of this isotypic series of zeolites allows us to identify common patterns of behaviour, which we attribute to the properties of the common ANA framework. The differences between the three structures must then be attributable to the different channel contents.

A noteworthy feature of our results is that the capacity for tetragonal distortions away from the perfectible cubic framework in analcime is very limited (as seen in Fig. 4). Leucite, however, displays a tetragonal framework at a markedly lower cell volume than analcime, which we find to be perfectible. This demonstrates that the flexibility window for the tetragonal framework as in leucite is not simply connected to the flexibility window for the cubic framework. As we reported in Sartbaeva *et al*. (2008), the connection between the perfectible cubic and triclinic frameworks in analcime is also not simple; linear interpolation between the cell parameters of the cubic and triclinic forms on either side of the phase transition does not yield perfectible structures.

The full flexibility window of a framework is a volume in the six-dimensional phase space defined by six independent cell parameters. The results we have obtained on the ANA framework strongly suggest that this volume may be neither simply connected nor highly symmetric, which has important implications regarding the difficulty of determining its extent. It has previously been observed in the modelling of rigid-unit modes in reciprocal space (for example, Pryde *et. al*., 1996) that the loci of wave vectors where rigid-unit modes exist can form exotic curved surfaces without obvious connections to the symmetry of the structure.

6 Theoretical: folding mechanisms in the ANA framework

The simulations of the cubic ANA framework under varying degrees of compression, which we performed to investigate the flexibility window, also provide information on the structural response of the framework to compression in terms of polyhedral tilting and collective motion. In our previous studies on zeolites (Gatta & Wells, 2004, 2006) we observed relatively simple compression behaviour based on the rotation of SBUs about the unique axis. The behaviour of the cubic ANA framework, by contrast, is more similar to that of dense high-symmetry silicates such as beta-quartz (Tucker *et al*., 2001; Sartbaeva *et al*, 2004). In this case the framework has a very large number of collective polyhedral tilting modes and as a result the instantaneous local structure can differ markedly from the average long-range structure seen in the crystal-structure refinement. We note that the geometric simulations are performed without symmetry restrictions on the atomic positions within the unit cell, and as a result we are able to observe these local variations.

The character of our results is illustrated in Fig. 6. Here we show three 6 mRs taken from a single unit cell of the cubic ANA framework under a slight degree of compression (cell parameter $a = 13.6$ Å). Recall, by comparison to Fig. 1, that in the average structure all such rings are symmetry constrained to be regular hexagonal rings. In the simulation we can see that each of the rings is a different and irregular shape reminiscent of the distorted rings seen in the leucite and wairakite structures.

In beta-quartz, it has been shown (Tucker *et al*., 2001) that the high-symmetry hexagonal average crystal structure is in fact a dynamic average. The instantaneous local structure contains significant deviations from hexagonal symmetry achieved by cooperative polyhedral tilting

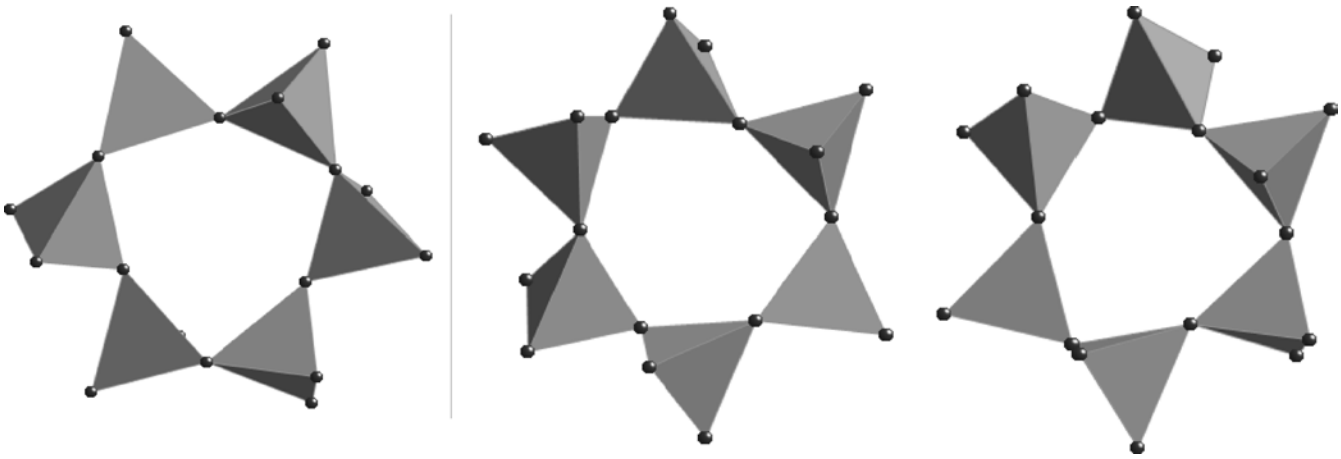

Fig. 6. Examples of 6-membered rings (6 mRs) from the ANA framework simulated with cubic cell parameters with $P1$ symmetry under a small degree of compression. The crystallographic symmetry of cubic analcime would require the 6 mRs to be regular as in Fig. 1, ''analcime''. However, here we see a large variation in the shapes of 6 mR units due to framework flexibility.

modes (Wells *et al.*, 2002) such that the local structure is more similar to low-symmetry alpha-quartz. Our simulation results strongly suggest that cubic analcime displays the same behaviour, and we therefore propose that the highly-symmetric cubic crystal structure with its symmetric regular 6 mRs is in fact a dynamic average over less symmetric local structures.

The very different asymmetric distortions of the 6 mRs in Fig. 6 arise from the fact that at the start of the geometric simulation we introduce a small random perturbation of all the atomic positions. In simulations beginning with different random seeds each 6 mR folds differently and no single uniform folding mechanism can be identified. It thus appears that the cubic analcime structure has a very large number of competing folding modes, while the displacive transition to the triclinic analcime structure under pressure corresponds to the selection of a single folding mode across the whole structure. On this basis we can account for the dramatic three-fold reduction in bulk modulus at the cubic to triclinic transition. In the cubic phase multiple incompatible local modes are in competition with each other, in the triclinic phase the entire structure follows one polyhedral tilting mode. This model, in which the higher-symmetry structures have competing folding modes, thus accounts for the softening of all three structures in their high-pressure phases with the effect being particularly dramatic for cubic analcime.

7. Discussion and conclusion

The experimental data collected at HP-conditions show that analcime, leucite and wairakite maintain their crystallinity at least up to 7–8 GPa, and any P-induced structural evolution is completely reversible within the P-range investigated. All the three isotypic feldspathoids undergo a P-induced phase-transition from high-to-low symmetry form: analcime at ~1 GPa (from $Ia\bar{3}d$ to $P\bar{1}$ symmetry); leucite between 2.2–2.8 GPa (from $I4_1/a$ to $P\bar{1}$ symmetry), and wairakite between 2.5–3.2 GPa (from $I2/a$ to $P\bar{1}$ symmetry). No further phase-transition was observed within the P-range investigated. For analcime and leucite, the P-induced transition is clearly a first-order transition, whereas for wairakite the order of the transition cannot be unambiguously defined because of the low quality of the powder data. On the basis of the structure refinements of the low-P and high-P polymorphs of analcime (Gatta *et al.*, 2006), and of the structural homologies of these feldspathoids, we suggest that P-induced phase-transitions in all the three isotypic minerals are displacive in character. The phase-transitions lead to a drastic increase in density in analcime and leucite (Gatta *et al.*, 2006, 2008). The extra-framework population seems to control the transition pressure. However, there is not a simple relationship between transition pressure and any parameter aimed to represent the extra-framework population (*e.g.*, ionic radius of the extra-framework cation or its polyhedral volume), likely because the configuration of the extra-framework content among these isotypic minerals is significantly different (*i.e.*, $NaO_4(H_2O)_2$ octahedron in cubic analcime; KO_6 in tetragonal leucite, with the K-sites located at the same positions of the H_2O-molecules oxygens in analcime; $CaO_4(H_2O)_2$ octahedron in monoclinic wairakite, with a configuration similar to that of analcime).

Analysis of the framework properties in terms of the ''flexibility window'' provides an explanatory framework for the nature of these phase transitions. For cubic analcime we were able to show that the observed range of densities is bracketed by the theoretical extent of the flexibility window for the cubic ANA structure, indicating that the transition to the low-symmetry form is induced by the structure approaching the high-density limit of its flexibility window. Leucite displays a similar behaviour, with the framework being perfectible in the tetragonal form at

all observed densities and then becoming intrinsically distorted after the transition to the low-symmetry form. The behaviour of wairakite is less clear, but we again find that the structure at ambient conditions and low pressures has a perfectible framework.

The elastic analysis shows that the H*P*-polymorphs of all the three feldspathoids are systematically more compressible than the low-*P* ones. In analcime, for example, the H*P*-triclinic polymorph is three times more compressible than the low-*P* cubic structure (Table 1). Less drastic are the differences in compressibility observed for low- and high-*P* polymorphs of leucite and wairakite (Table 1). An increase in compressibility of the H*P* polymorph with respect to the low-*P* one is ''anomalous'' but not unique, as it was already observed in other classes of natural materials (*e.g.*, sheet silicates, Welch *et al*., 2004, and carbonates, Merrill & Bassett, 1972, 1975; Singh & Kennedy, 1974; Martinez *et al*., 1996; Smyth & Ahrens, 1997; Redfern, 2000; Holl *et al*., 2000). For analcime, the compression behaviour of the H*P*-polymorph is better described with a third-order BM-EoS. The value of the bulk modulus pressure-derivative [*i.e.*, $K' = 6.8(7)$, Fig. 2 and 3, Table 1] shows that a significant change in compressibility with pressure occurs. In contrast, for leucite and wairakite a second-order BM-EoS is sufficient to describe the compression regime for the low- and high-*P* polymorphs, with the K' fixed to four (Fig. 2 and 3, Table 1). A further point concerns the elastic anisotropy among the three feldspathoids. For triclinic analcime, the elastic anisotropy is significant, being $K_a{:}K_b{:}K_c = 2.64{:}1.82{:}1$. On the basis of the structural refinements of the H*P*-triclinic polymorph of analcime at different pressures, Gatta *et al.* (2006) were able to explain the reason of the elastic anisotropy, mainly driven by the rearrangement of the SBU (4 mR and 6 mR). In leucite, it is interesting to point out that the low-*P* tetragonal polymorph is elastically more anisotropic than the high-*P* triclinic one, being $K_a{:}K_b{:}K_{c(\text{tetragonal})} = 1{:}1{:}2.26$ and $K_a{:}K_b{:}K_{c(\text{triclinic})} = 1.03{:}1{:}1.02$. It appears, therefore, that the atomic relaxation at pressure above the phase-transition leads to a structure more stable as a function of pressure than the low-*P* one. In wairakite, the low-*P* monoclinic polymorph is significantly anisotropic, but the high-*P* triclinic form is drastically more anisotropic, being $K_a{:}K_b{:}K_{c(\text{monoclinic})} = 1.38{:}2.69{:}1$ and $K_a{:}K_b{:}K_{c(\text{triclinic})} = 2.92{:}6.11{:}1$.

The geometric simulations capturing the nature of the flexibility of the ANA framework suggest an explanation for the anomalous elastic behaviour. We suggest that the symmetry-restricted atomic positions found for cubic analcime are in fact dynamic averages over lower-symmetry instantaneous structures. This behaviour is not unusual for high-symmetry framework silicates, as for example in the case of beta-quartz. The high-symmetry cubic framework is rich in flexible modes and can ''fold'' in many competing and incompatible ways. The transition from the cubic to the triclinic form corresponds to the selection of a single dominant folding mode which breaks the average symmetry of the framework.

Acknowledgements: Financial support to GGD was provided by MIUR Project 2006040119_004. AS thanks Glasstone Research Fellowship and SAW thanks Leverhume Trust for financial support. W. Crichton and an anonymous reviewer are thanked.

References

Angel, R.J. (2000): Equation of state. *in* ''High-temperature and high-pressure crystal chemistry'', Hazen, R.M. & Downs, R.T., eds. Rev. Miner. Geochem., **41**, 35–59, Mineralogical Society of America and Geochemical Society, Washington, DC.

Angel, R.J. (2001): EOS-FIT V6.0. Computer program. Crystallography Laboratory, Dept. Geological Sciences, Virginia Tech, Blacksburg.

Armbruster, T. & Gunter, M.E. (2001): Crystal structures of natural zeolites. *in* ''Natural zeolites: occurrence, properties, application'', Bish, D.L. & Ming, D.W., eds. Rev. Miner. Geochem., **45**, 1–57, Mineralogical Society of America and Geochemical Society, Washington, DC.

Baerlocher, Ch., Meier, W.M., Olson, D.H. (2001): Atlas of zeolite framework types, 5th edn. Elsevier, Amsterdam, NL, 302 p.

Birch, F. (1947): Finite elastic strain of cubic crystal. *Phys. Rev*., **71**, 809–824.

Coombs, D.S., Alberti, A., Armbruster, T., Artioli, G., Colella, C., Galli, E., Grice, J.D., Liebau, F., Mandarino, J.A., Minato, H., Nickel, E.H., Passaglia, E., Peacor, D.R., Quartieri, S., Rinaldi, R., Ross, M., Sheppard, R.A., Tillmanns, E., Vezzalini, G. (1997): Recommended nomenclature for zeolite minerals: report of the Subcommittee on Zeolites of International Mineralogical Association, Commission on new minerals and minerals names. *Can. Mineral.*, **35**, 1571–1606.

Deer, W.A., Howie, R.A., Zussman, J. (2004): Rock-forming minerals, Vol. 4B: Framework silicates. The Geological Society, London.

Ferraris, G., Jones, D.W., Yerkess, J. (1972): A neutron-diffraction study of the crystal structure of analcime, $NaAlSi_2O_6{\cdot}H_2O$. *Z. Kristallogr*., **135**, 240–252.

Gatta, G.D. & Wells S.A. (2004): Rigid unit modes at high pressure: an explorative study of a fibrous zeolite-like framework with EDI topology. *Phys. Chem. Minerals*, **31**, 465–474.

Gatta, G.D., Nestola, F., Boffa Ballaran, T. (2006): Elastic behavior, phase transition and pressure induced structural evolution of analcime. *Am. Mineral.*, **91**, 568–578.

Gatta, G.D. & Wells S.A. (2006): Structural evolution of zeolite levyne under hydrostatic and non-hydrostatic pressure: geometric modelling. *Phys. Chem. Minerals*, **33**, 243–255.

Gatta, G.D., Rotiroti, N., Bellatraccia, F., Della Ventura, G. (2007): Crystal-chemistry of leucite from the Roman Comagmatic Province (Central Italy); a multi-methodological study. *Mineral. Mag*., **71**, 593–604.

Gatta, G.D., Rotiroti, N., Boffa Ballaran, T., Pavese A. (2008): Leucite at high-pressure: elastic behaviour, phase stability and petrological implications. *Am. Mineral.*, **93**, 1588–1596.

Gianpaolo, C., Godano, R.F., Di Sabatino, B., Barrese, E. (1997): The alteration of leucite-bearing rocks: a possible mechanism. *Eur. J. Mineral*., **9**, 1293–1310.

Gottardi, G. & Galli, E. (1985): Natural zeolites. Springer-Verlag, Berlin, 409 p.

Hazen, R.M. & Finger, L.W. (1979): Polyhedral tilting: a common type of pure displacive phase transition and its relationship to analcime at high pressure. *Phase Transitions*, **1**, 1–22.

Heinz, D.L. & Jeanloz, R. (1984): The equation of state of the gold calibration standard. *J. Appl. Phys*., **55**, 885–893.

Holl, C.M., Smyth, J.R., Laustsen, H.M.S., Jacobsen, S.D., Downs, R.T. (2000): Compression of witherite to 8 GPa and the crystal structure of $BaCO_3$-II. *Phys. Chem. Minerals*, **27**, 467–473.

Luhr, J.F. & Kyser, T.K. (1989): Primary igneous analcime: the Colima minettes. *Am. Mineral*., **74**, 216–223.

Mazzi, F., Galli, E., Gottardi, G. (1976): The crystal structure of tetragonal leucite. *Am. Mineral*., **61**, 108–115.

Mazzi, F. & Galli, E. (1978): Is each analcime different? *Am. Mineral*., **63**, 448–460.

Martinez, I., Zhang, J., Reeder, R.J. (1996): In-situ X-ray diffraction of aragonite and dolomite at high pressure and high temperature: evidence for dolomite breakdown to aragonite and magnesite. *Am. Mineral*., **81**, 611–624.

Merrill, L. & Bassett, W.A. (1972): Crystal structures of the high pressure phases of calcite. *EOS*, **53**, 1121.

Merrill, L. & Bassett, W.A. (1975): The crystal structure of $CaCO_3$ (II), a high pressure metastable phase of calcium carbonate. *Acta Crystallogr*., **B31**, 343–349.

Ori, S., Quartieri, S., Vezzalini, G., Dmitriev, V. (2008): Pressure-induced structural deformation and elastic behavior of wairakite. *Am. Mineral*., **93**, 53–62.

Passaglia, E. & Sheppard, R.A. (2001): The crystal chemistry of zeolites. *in* ''Natural zeolites: occurrence, properties, application'', Bish, D.L. & Ming, D.W., eds. Rev. Miner. Geochem., **45**, 69–116, Mineralogical Society of America and Geochemical Society, Washington, DC.

Peccerillo, A. (1998): Relationships between ultrapotassic and carbonate-rich volcanic rocks in central Italy: petrogenetic and geodynamic implications. *Lithos*, **43**, 267–279.

Peccerillo, A. (2003): Plio-Quaternary magmatism in Italy. *Episodes*, **26**, 222–226.

Peccerillo, A. (2005): Plio-Quaternary volcanism in Italy. Petrology, Geochemistry, Geodynamics. Springer, Heidelberg, Germany, 365 p.

Prelević, D., Foley, S.F., Cvetković, V., Romer, R.L. (2004): The analcime problem and its impact on the geochemistry of ultrapotassic rocks from Serbia. *Mineral. Mag*., **68**, 633–648.

Redfern, S.A.T. (2000): Structural variations in carbonates. *in* ''High-temperature and high-pressure crystal chemistry'', Hazen, R.M. & Downs, R.T., eds. Rev. Miner. Geochem., **41**, 289–308, Mineralogical Society of America and Geochemical Society, Washington, U.S.A.

Redkin, A.F. & Hemley, J.J. (2000): Experimental Cs and Sr sorption on analcime in rock-buffered systems at 250–300 °C and Psat and the thermodynamic evaluation of mineral solubilities and phase relations. *Eur. J. Mineral.*, **12**, 999–1014.

Roux, J. & Hamilton, D. (1976): Primary igneous analcime; an experimental study. *J. Petrology*, **17**, 244–257.

Pryde, A.K.A., Hammonds, K.D., Dove, M.T., Heine, V., Gale, J.D., Warren, M.C. (1996): Origin of the negative thermal expansion in ZrW_2O_8 and ZrV_2O_7. *J. Phys. Cond. Matt.*, **50**, 10973–10982.

Sartbaeva, A., Wells, S.A., Redfern, S.A.T. (2004): Li^+ ion motion in quartz and beta-eucryptite studied by dielectric spectroscopy and atomistic simulations. *J. Phys. Cond. Matt.*, **16**, 8173–8189.

Sartbaeva, A., Wells, S.A., Redfern, S.A.T., Hinton, R.W., Reed, S.B.J. (2005): Ionic transport in quartz studied by transport measurements, SIMS and atomistic simulations, *J. Phys. Cond. Matt.*, **17**, 1099–1112.

Sartbaeva, A., Wells, S.A., Treacy, M.M.J., Thorpe, M.F. (2006): The flexibility window in zeolites. *Nature Mat.*, **5**, 962–965.

Sartbaeva, A., Gatta, G.D., Wells, S.A. (2008): Flexibility window controls compression behaviour in analcine zeolite framework. *Europhysics Lett.*, **83**, 26002.

Singh, A.K. & Kennedy, G.C. (1974): Compression of calcite to 40 kbar. *J. Geophys. Res.*, **79**, 2615–2622.

Smyth, J.R. & Ahrens, T.J. (1997): The crystal structure of calcite III. *Geophys. Res. Lett.*, **25**, 1595–1598.

Tucker, M.G, Dove, M.T., Keen, D.A. (2001): Application of the reverse Monte Carlo method to crystalline materials. *J. Appl. Cryst.*, **34**, 630–638.

Takeuchi, Y., Mazzi, F., Haga, N., Galli, E. (1979): The crystal structure of wairakite. *Am. Mineral.*, **64**, 993–1001.

Tschernich, R.W. (1992): Zeolites of the world. Geoscience Press Inc., Phoenix, Arizona.

Welch, M.D., Kleppe, A.K., Jephcoat, A.P. (2004): Novel high-pressure behavior in chlorite: a synchrotron XRD study of clinochlore to 27 GPa. *Am. Mineral.*, **89**, 1337–1340.

Wells, S.A., Dove, M.T., Tucker, M.G., Trachenko, K. (2002): Real-space rigid-unit-mode analysis of dynamic disorder in quartz, cristobalite and amorphous silica. *J. Phys. Cond. Matt.*, **14**, 4645–4657.

Wells, S.A., Dove, M.T., Tucker, M.G. (2004): Reverse Monte Carlo with geometric analysis – RMC + GA. *J. Phys. Cond. Matt.*, **37**, 536–544.

Wells, S.A., Menor, S, Hespenheide, B, Thorpe, M.F. (2005): Constrained geometric simulation of diffusive motion in proteins. *Phys. Biolog*., **2**, S127-S136.

Wilkinson, J.F.G. (1977): Analcime phenocrysts in a vitrophyric analcimite; primary or secondary? *Contrib. Mineral. Petrol*., **64**, 1–10.

Woolley, A.R. & Symes, R.F. (1976): The analcime-phyric phonolites (blairmorites) and associated analcime kenytes of the Lupata Gorge, Mocanbique. *Lithos*, **9**, 9–15.

Received 19 August 2008
Modified version received 15 December 2008
Accepted 12 January 2009